

SERRA DA CANGALHA, TOCANTINS, BRAZIL: INSIGHTS TO THE STRUCTURE OF A COMPLEX IMPACT CRATER WITH AN OVERTURNED CENTRAL UPLIFT. T. Kenkmann¹, M. Vasconcelos², A. P. Crósta² and W.U. Reimold¹, ¹ Museum für Naturkunde, Leibniz Institut at Humboldt-University Berlin, Thomas.kenkmann@mfn-berlin.de, ²Institute of Geosciences, University of Campinas, Campinas, SP, Brazil

Introduction: Serra da Cangalha in Brazil (8°5'S/46°52'W) was proposed as a possible impact structure because of its circular shape [1] and possible shatter cone occurrences [1-3]. A recent remote sensing study [4] revealed its great potential for structural analysis. Here we present results of a mapping campaign in the impact crater in May 2009.

Methods: In the course of the field campaign 442 GPS referenced data points were taken with notation of lithology, bedding plane orientation and structure. The declination correction is -19°. Errors on GPS coordinates are usually 6 m, on strata orientations 5°. For mapping purposes we also used geo-referenced CBERS-2B/HRS (2.7 m res.) and WorldView-1 (0.5 m res.) satellite images. Geologic surveying and mapping were performed utilizing the ArcGIS 9.3 software package by ESRI. Geographic coordinates for data-points, faults, and lineaments were transformed into radial coordinates to analyse concentric deviations and distances from the crater center. For details of data conversion and notations see [5].

Morphometry: The crater rim can be delineated from satellite images and ranges in diameter from 13400 to 14000 m, (mean Ø: 13730 m). The region outside the crater is represented by a table mountain land dissected by fluvial drainage systems. The crater rim is a concentrically trending monocline, whose inner limb dips towards the crater center. The moat between crater rim and central uplift is a depressed region with a concentric drainage system and subdued

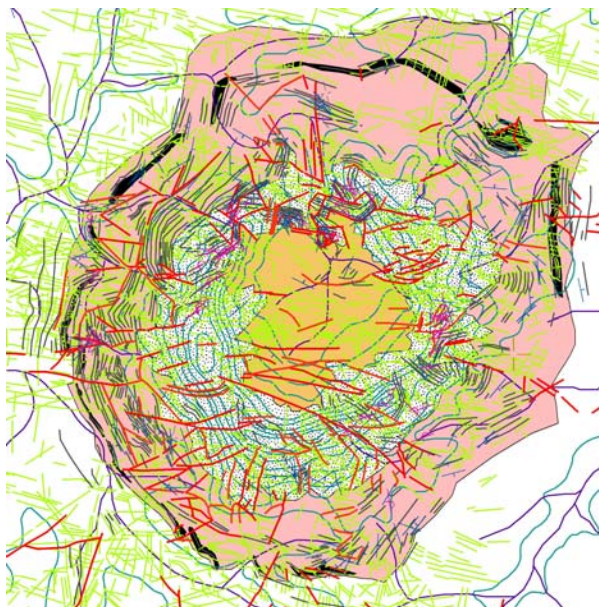


Fig. 1 Geological map of the central uplift of Serra da Cangalha

ring features [4]. The central uplift (Fig. 1) has a diameter of 5300 to 6500 m (mean Ø: 5800 m). The 200-300 m high collar of the central uplift is 2650-3075 m in diameter (mean Ø = 2830 m). The collar has a somewhat quadrangular shape with an open part to the NNW. The central uplift is off-set to the WSW by ~550 m from the geometric crater center defined by the crater rim.

Stratigraphy: The lowermost stratigraphic unit is formed by dark claystone of Devonian age (Longá Fm.) outcropping in the center (Fig.1; beige). They are surrounded by Carboniferous sandstones (Poti Fm; Fig. 1 stippled, Fig. 2), forming the collar of the central uplift. Piauí Fm. (Fig. 1 rosè) forms the periphery of the central uplift. The uppermost stratigraphic unit is the Pedra de Fogo Fm. mostly com sandstones.



Fig. 2 a. Collar of the central uplift with overturned beds of Poti sandstone and steeply plunging radial folds.

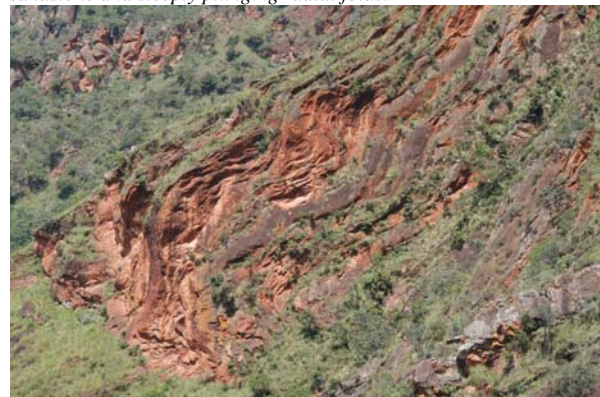


Fig. 2b Folding of overturned Poti sandstone of the collar with horizontal axes indicating gravitational instability.

Shock features: A few shatter cones and rare monomict and polymict breccias were found in the central depression. Breccias along with some sandstones from the central uplift contain shocked quartz grains with planar deformation features (PDFs), planar

fractures (PFs), and feather features (FFs) as unequivocal evidence for an impact origin. Chert breccias are frequent in the central uplift periphery (Fig.1, black). These steeply-inclined, stratiform breccias are of diagenetic origin and not impact-derived. They belong to the Piauí Fm. and form morphological ridges in the circumference of the central uplift.

Joint lineaments: Joint and cleavage planes were mapped on CBERS-2B/HRS images inside and outside the crater. They partly control the shape of escarpments and monadnocks, and influence the density of the vegetation cover. The statistical analysis is based on more than 6200 digitized data. The lineaments dominantly trend 102° (ESE-WNW) and 12° (NNE-SSW) both inside and outside the crater (Figs. 1, 3). However, within the crater the variability of orientations is enhanced. Joints at 102° and 12° trends are of pre-impact origin (see below) but also superimposed on impact-induced features indicating a stable tectonic stress field that existed prior to and persisted after the impact.

Faults: We mapped 435 faults of variable offset. Radial faults dominate over concentric ones (Fig. 4). E-W striking faults are dominant (Fig.1) and particularly occur in the E and W sectors of the central uplift where they form imbricated stacks of blocks. The presence of E-W striking faults (95°) and, to a lesser degree, of NNE striking impact faults (15°) suggests that the regional joint system must have existed prior to impact.

Bedding and folding: Statistical analysis of bedding plane orientations shows that they dominantly strike concentrically (Fig. 5). However, deviation from concentric strike increases with decreasing distance from the center (Fig.1). Deviations are strongest and of opposite sign (30° on average) in the SSE and SW part of the collar of the central uplift. Outside the crater beds usually lie flat. Along the inner limb of the crater rim monocline, gentle dips towards the crater interior were found. Within the crater moat limited outcrops hinder a proper analysis. The central uplift is defined by the sudden appearance of vertical beds (chert breccia, Fig. 1, black). The complete S and W collar comprises overturned beds. These beds are folded in an interference pattern: One fold system has steeply plunging radial axes (Fig. 2a), the other has concentric, horizontal axes (Fig. 2b). Both were formed during central uplift formation. The former is a spatial requirement during inward flow and central uplift formation – a phenomenon known from many complex impact craters. The latter indicates the instability and onset of gravitational collapse of the central uplift under its own weight.

Conclusion: The gravitational instability of the central uplift might result from the target’s rheological stratification with claystone exposed in the center. Pre-existing joint systems substantially controlled the movements during crater collapse.

References: [1] Dietz R. S. & French B. M. (1973). *Nature* 244:561. [2] McHone (1979) NASA Spec. Pub. SP-412. pp 193–202. [3] Crosta A. P. (1987). In Pohl J (ed.) *Research in Terrestrial Impact Structure*, 30-38. [4] Reimold W.U. et al. (2006) *MAPS*, 41: 237. [5] Poelchau M. H. & Kenkmann T. (2008) *MAPS* 43, 2058.

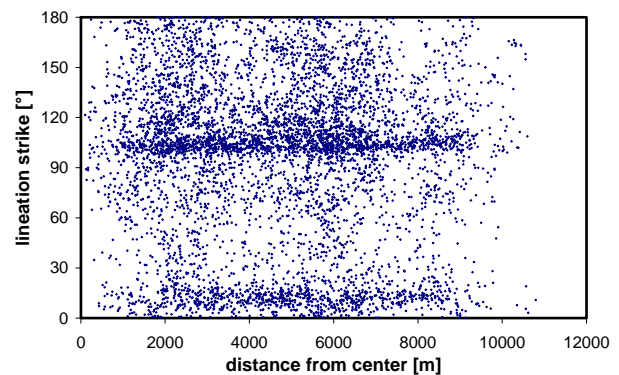


Fig.3 Strike of lineaments vs. distance from crater center.

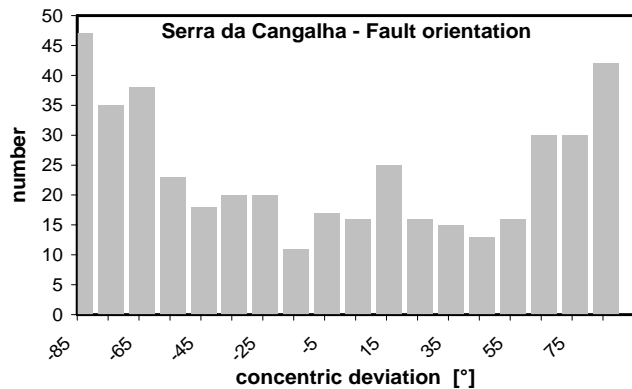


Fig. 4 Histogram of fault orientation within the crater.

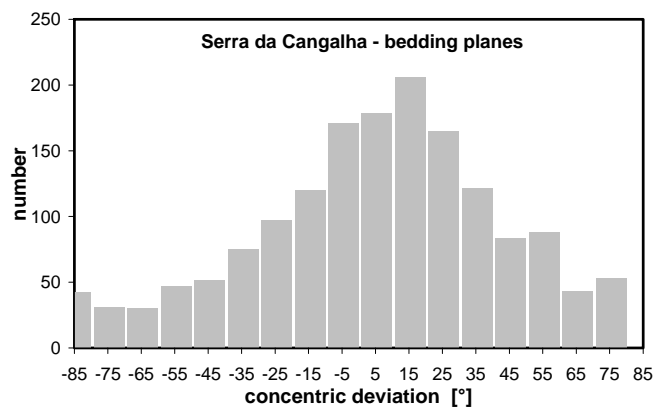


Fig.5 Histogram of the orientation of bedding planes.